

# Monte Carlo simulation of localization dynamics of excitons in ZnO and CdZnO quantum well structures

T. Makino<sup>a)</sup>

Department of Material Science, University of Hyogo, Kamigoori 672-1297, Japan

K. Saito

Department of Physics, The University of Tokyo, Tokyo 113-0033, Japan

A. Ohtomo and M. Kawasaki

Institute for Materials Research, Tohoku University, Sendai 980-8577, Japan

R. T. Senger

Department of Physics, Bilkent University, 06800 Ankara, Turkey

K. K. Bajaj

Department of Physics, Emory University, Atlanta, Georgia 30322

(Received 11 January 2006; accepted 7 February 2006; published online 27 March 2006)

Localization dynamics of excitons was studied for ZnO/MgZnO and CdZnO/MgZnO quantum wells (QWs). The experimental photoluminescence (PL) and absorption data were compared with the results of Monte Carlo simulation in which the excitonic hopping was modeled. The temperature-dependent PL linewidth and Stokes shift were found to be in a reasonable agreement with the hopping model, with accounting for an additional inhomogeneous broadening. The density of localized states used in the simulation for the CdZnO QW was consistent with the absorption spectrum. © 2006 American Institute of Physics. [DOI: [10.1063/1.2181431](https://doi.org/10.1063/1.2181431)]

Recently, there have been extensive studies on optical properties of semiconductor quantum structures.<sup>1</sup> In particular, II-VI oxides have attracted a great deal of attention owing to the fact that their excitons have large binding energies.<sup>2,3</sup> The recent success of *p*-type doping<sup>2,3</sup> has opened a door to realize application of ultraviolet (UV) light-emitting diodes. Introduction of cadmium and/or magnesium into ZnO plays a key role in strain<sup>4</sup> and band engineering of these oxides.<sup>5,6</sup> In previous work, we have reported an S-shaped temperature dependence of the photoluminescence (PL) in ZnO/MgZnO and CdZnO/MgZnO quantum wells (QWs).<sup>7–9</sup>

Here, we report the W-shaped dependence of the PL.<sup>10</sup> We model these temperature behaviors of the emission band and compare the results with the experimental data. We use a Monte Carlo simulation which is based on the excitonic kinetics.<sup>10</sup>

The samples were ZnO and CdZnO QWs. Both of these QWs were grown with laser molecular-beam epitaxy on ScAlMgO<sub>4</sub> substrates. The material of our barrier layers is 5-nm-thick Mg<sub>x</sub>Zn<sub>1-x</sub>O. The PL was studied in the temperature range from 5 to 300 K. The continuous-wave He-Cd laser was used.<sup>11</sup>

The luminescence spectra taken for the ZnO/Mg<sub>0.27</sub>Zn<sub>0.73</sub>O QW (the well width being 1.8 nm) exhibit a double band<sup>8,12</sup> at intermediate temperatures of 95–175 K. Figure 1 shows a typical PL spectrum at 120 K. These two emission bands correspond to radiative recombination of localized excitons (LX<sub>1</sub> and LX<sub>2</sub>). The temperature dependence of the peak (see also Fig. 2 of Ref. 8) exhibits a well-

known S-shaped variation.<sup>8</sup> The initial redshift reflects the ability of localized excitons to reach lower-energy sites via thermally activated hopping. The blueshift and the splitting of peaks that are observed with further increase in temperature may be attributed to the population of the localized exciton states with increasingly higher energy.

The features of hopping of localized excitons are supported by the linewidth and Stokes shift measurements. The points in Figs. 2(a) and 2(b) show temperature variations of the full width at half maximum (FWHM) and Stokes shift of the PL band. Here, we notice a W-shaped temperature dependence<sup>10</sup> of the linewidth. Its abrupt increase with temperature (5–100 K) was related to thermalization of the excitons over localized states, as opposed to the situation at

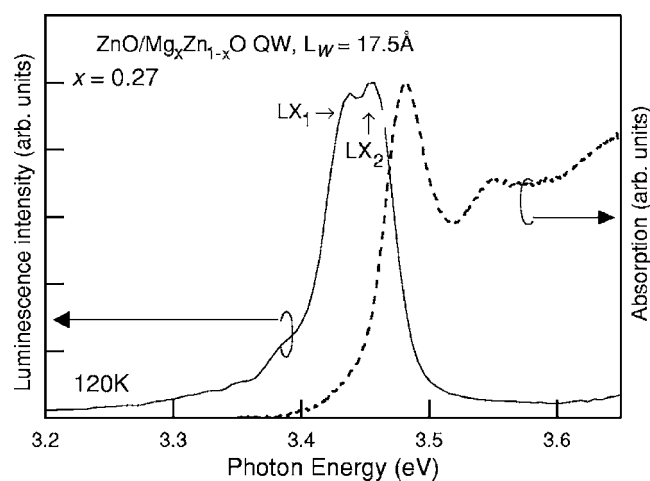


FIG. 1. The excitonic absorption and PL spectra in a ZnO/Mg<sub>0.27</sub>Zn<sub>0.73</sub>O MQW (well width being 1.8 nm) taken at 120 K.

<sup>a)</sup>Electronic mail: makino@sci.u-hyogo.ac.jp

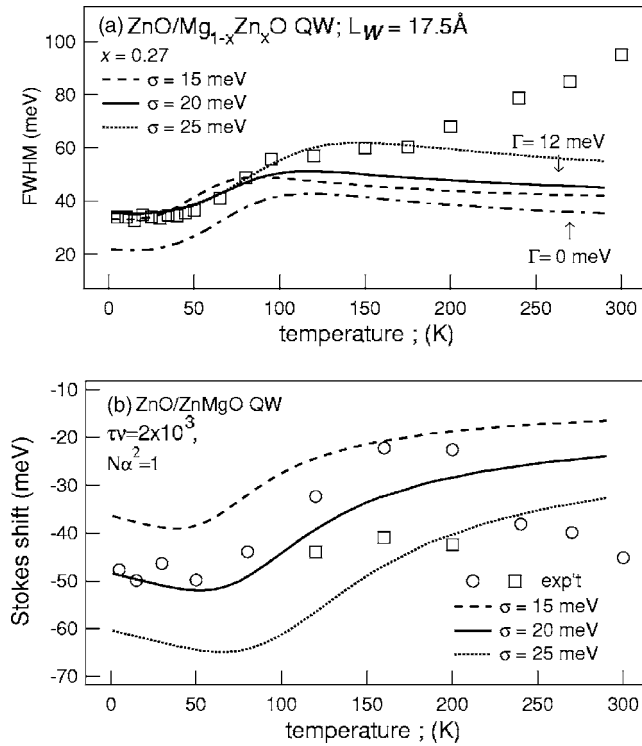


FIG. 2. (a) Evolution of the FWHM of the PL band with temperature. Open squares show experimental data; dashed, dotted, and solid lines depict results of the simulation for different scales of random potential fluctuations  $\sigma$  (indicated) with the inhomogeneous broadening  $\Gamma$ ; and the dash-dotted line represents results for  $\sigma=20$  meV and  $\Gamma=0$ . (b) Simulated and experimental temperature dependences of the Stokes shifts.

lower temperatures where the excitons do not attain their equilibrium distribution. On the other hand, the temperature variation of Stokes shift is more complicated due to the peak splitting at the intermediate temperatures.

The temperature dependences were simulated by a two-dimensional (2D) Monte Carlo algorithm. This algorithm adopts the Miller-Abrahams rate for phonon-assisted exciton tunneling between initial and final states ( $i$  and  $j$ ) with the energies of  $\epsilon_i$  and  $\epsilon_j$ , respectively,<sup>10</sup>

$$\nu_{ij} = \nu_0 \exp\left(-\frac{2r_{ij}}{\alpha} - \frac{\epsilon_i - \epsilon_j + |\epsilon_i - \epsilon_j|}{2kT}\right). \quad (1)$$

Here  $r_{ij}$  is the distance between the localization sites,  $\alpha$  is the decay length of the exciton wave function, and  $\nu_0$  is the attempt-escape frequency. Hopping was simulated over a randomly generated set of localized states with the sheet density of  $N$ . Density of states (DOS) of the localization energies was assumed to be in accordance with a Gaussian distribution,

$$g(\epsilon) = (N^2/2\pi\sigma^2)^2 \exp[-(\epsilon - E_0)^2/2\sigma^2], \quad (2)$$

with the peak positioned at the mean excitonic energy  $E_0$  and the dispersion parameter (the energy scale of the band potential profile fluctuation)  $\sigma$ . The reference energy was  $\epsilon=E_0$ , which is the center of the distribution. All the energies in our simulation were below this value, i.e., a “half” distribution.<sup>13</sup> For each generated exciton, the hopping process terminates by recombination with the probability  $\tau_0^{-1}$  and the energy of the localized state is scored to the emission spectrum.

The temperature variation of the data is basically determined by the spatial (the product  $N\alpha^2$ ) and temporal (the product  $\tau_0\nu_0$ ) parameters. For example, the kink in the temperature dependence of the FWHM is related to the energy of the potential fluctuations  $\sigma$ , i.e.,  $\sigma=2k_B T_{\text{kink}}$  (Refs. 10 and 14).

It has been difficult to reproduce both of our FWHM and energy shifting behaviors with the identical set of simulation parameters. Nevertheless, if we adopt the values of  $N\alpha^2=1$ ,  $\tau_0\nu_0=2 \times 10^3$ , and  $\sigma=20$  meV, the calculated result approximately reproduces the 22 meV amplitude of the variation of FWHM curve as shown by a solid curve in Fig. 2(a). The dashed and dotted lines in Fig. 2(a) demonstrate the sensitivity of the simulated results with respect to the hopping energy scale  $\sigma$ . Increased  $\sigma$  matches better with the experiment, but, as explained later, we will meet serious difficulty in accommodating the experimental Stokes shifts. The quantitative agreement with the experimental data requires an additional inhomogeneous broadening ( $\Gamma=12$  meV) to be introduced.<sup>10</sup> The dash-dotted line shows the simulated dependence without inhomogeneous broadening ( $\Gamma$ ). The further increase of the linewidth above 175 K is attributed to the participation of the longitudinal optical phonons in the radiative transition not accounted for in the model.

The temperature behavior of the Stokes shift is depicted in Fig. 2(b). The following feature was reproduced in the simulated results: the crossover temperature for the energy minimum in the S-shaped dependence (50–60 K). On the other hand, the initial redshifting behavior at low temperatures is somewhat exaggerated. We can accommodate this disagreement if the value of  $\tau_0\nu_0$  is reduced. But, the agreement for the FWHM becomes worse. More refinement of the model should be necessary to describe this splitting. Nevertheless, it is thought that the simulated Stokes shift energies correspond to the average energy of the splitted peaks. At temperatures higher than 230 K, the experimental data of the Stokes shift are not in good agreement with those of the simulation. This is probably because the spectral weight moves to the direction of the emission peak of longitudinal-optical phonon replicated recombination at the elevated temperatures as has been pointed out for ZnO bulk crystals and thin films.<sup>15,16</sup>

For comparison, the simulated results for the  $\text{Cd}_{0.04}\text{Zn}_{0.96}\text{O}/\text{Mg}_{0.12}\text{Zn}_{0.88}\text{O}$  QW (the well width being 1.8 nm) were shown in Figs. 3(a) and 3(b). The solid line in Fig. 3(a) represents the best fit obtained for the following values of the parameters:  $N\alpha^2=1$ ,  $\tau_0\nu_0=7 \times 10^3$ ,  $\Gamma=29$  meV, and  $\sigma=20$  meV. Unfortunately, the experimental Stokes shift datum was obtained solely at 5 K. This is in a good agreement with the result of simulation as shown with the open circle in Fig. 3(b).

Finally, Fig. 4 compares the 5 K absorption spectrum (a dashed line) with the actual density of localized states used in the simulation (a solid line),

$$D(E) \propto \exp\left[\frac{-(E - E_0)^2}{2(\sigma^2 + \Gamma^2)}\right], \quad (3)$$

where the inhomogeneous broadening is taken into account by the introduction of  $\Gamma$  (here 29 meV). These densities of

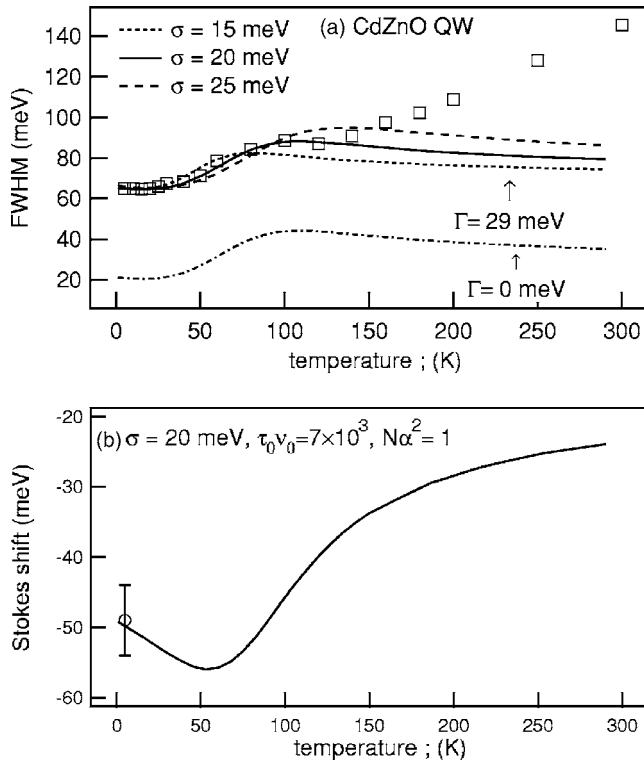


FIG. 3. Same as Fig. 2 except that the sample is now a  $\text{Cd}_{0.04}\text{Zn}_{0.96}\text{O}/\text{Mg}_{0.12}\text{Zn}_{0.88}\text{O}$  QW (well width being 1.8 nm).

band-tail states are centered at the exciton transition energy (3.285 eV) obtained by adding the *simulated* Stokes shift [Fig. 3(b)] with the *experimental* PL energy (see also Fig. 2 of Ref. 7). In addition, the long-wavelength wing of  $D(E)$  is seen to be in a fairly good coincidence with the low-energy tail of the corresponding absorption spectrum.

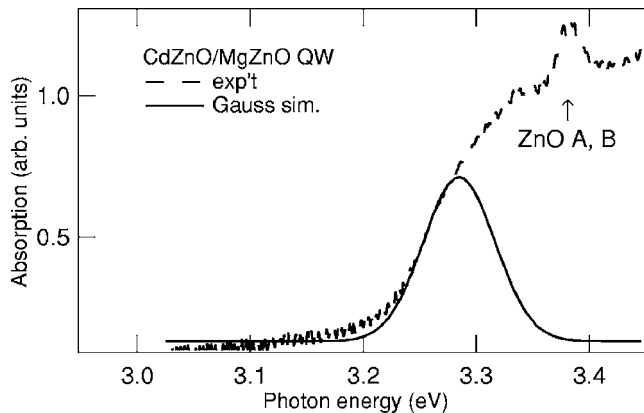


FIG. 4. Optical absorption spectrum (dashed line) of a CdZnO MQW taken at 5 K. A solid line shows the density of band-tail states used in the simulation with the inhomogeneous broadening ( $\Gamma$ ) accounted for. The most prominent peaks ("ZnO A, B") come from the ZnO buffer layer.

The value of  $\Gamma$  for the CdZnO QW (29 meV) is significantly larger than that for the ZnO QW (12 meV), which is not surprising because of the more severe inhomogeneity in the former sample; both the well and barrier layers are comprised of alloyed materials. Accordingly,  $\tau_0 \nu_0$  for the CdZnO QW is also larger. It is likely that the effective lifetime (related to  $\tau_0$ ) is longer.<sup>7</sup>

Here we try to evaluate precise Cd concentration at irradiated region of the sample from a variational calculation<sup>17</sup> where the electron-phonon interaction is taken into account. If the concentration is set to 4.3%, the transition energy is calculated to be 3.288 eV, which is very close to the exciton transition energy at 5 K.

In conclusion, we studied the evolution of the PL maximum and FWHM of ZnO QWs with temperature by the Monte Carlo simulation. By making efforts to reproduce both of FWHM and energy shift with the same set of parameters, the characteristic energy scale of the distribution of the localized states was  $\sigma \approx 20$  meV. The values of  $\Gamma$  and  $\tau_0 \nu_0$  for the CdZnO QW are significantly larger than those for the ZnO QW. The density of localized states employed in the simulation turned out to be in a good agreement with the long-wavelength region of the absorption spectrum.

The authors are thankful to Y. Segawa, N. T. Tuan, C. H. Chia, and Y. Takagi, for discussions. Thanks are also due to H. Koinuma.

- <sup>1</sup>A. L. Efros, M. Rosen, M. Kuno, M. Nirmal, D. J. Norris, and M. Bawendi, *Phys. Rev. B* **54**, 4843 (1996).
- <sup>2</sup>D. C. Look, D. C. Reynolds, C. W. Litton, R. L. Jones, D. B. Eason, and G. Cantwell, *Appl. Phys. Lett.* **81**, 1830 (2002).
- <sup>3</sup>A. Tsukazaki *et al.*, *Nat. Mater.* **4**, 42 (2005).
- <sup>4</sup>T. Makino, Y. Segawa, A. Ohtomo, K. Tamura, T. Yasuda, M. Kawasaki, and H. Koinuma, *Appl. Phys. Lett.* **79**, 1282 (2001).
- <sup>5</sup>T. Makino, Y. Segawa, M. Kawasaki, A. Ohtomo, R. Shiroki, K. Tamura, T. Yasuda, and H. Koinuma, *Appl. Phys. Lett.* **78**, 1237 (2001).
- <sup>6</sup>T. Makino, Y. Segawa, M. Kawasaki, and H. Koinuma, *Semicond. Sci. Technol.* **20**, S78 (2005).
- <sup>7</sup>T. Makino, N. T. Tuan, Y. Segawa, C. H. Chia, M. Kawasaki, A. Ohtomo, K. Tamura, and H. Koinuma, *Appl. Phys. Lett.* **77**, 1632 (2000).
- <sup>8</sup>T. Makino *et al.*, *Appl. Phys. Lett.* **78**, 1979 (2001).
- <sup>9</sup>T. Makino, C. H. Chia, K. Tamura, A. Ohtomo, M. Kawasaki, H. Koinuma, and Y. Segawa, *J. Appl. Phys.* **93**, 5929 (2003).
- <sup>10</sup>K. Kazlauskas *et al.*, *Appl. Phys. Lett.* **83**, 3722 (2003).
- <sup>11</sup>T. Makino, C. H. Chia, N. T. Tuan, Y. Segawa, M. Kawasaki, A. Ohtomo, K. Tamura, and H. Koinuma, *Appl. Phys. Lett.* **76**, 3549 (2000).
- <sup>12</sup>T. Makino, K. Tamura, C. H. Chia, Y. Segawa, M. Kawasaki, A. Ohtomo, and H. Koinuma, *Phys. Rev. B* **66**, 233305 (2002).
- <sup>13</sup>B. D. Don, K. Kohary, E. Tsitsishvili, H. Kalt, S. D. Baranovskii, and P. Thomas, *Phys. Rev. B* **69**, 045318 (2004).
- <sup>14</sup>R. Zimmermann, F. Grosse, and E. Runge, *Pure Appl. Chem.* **69**, 1179 (1997).
- <sup>15</sup>W. Shan, W. Walukiewicz, J. W. Ager III, K. M. Yu, H. B. Yuan, H. P. Xin, G. Cantwell, and J. J. Song, *Appl. Phys. Lett.* **8**, 191911 (2005).
- <sup>16</sup>T. Makino, Y. Segawa, S. Yoshida, A. Tsukazaki, A. Ohtomo, M. Kawasaki, and H. Koinuma, *J. Appl. Phys.* **98**, 093520 (2005).
- <sup>17</sup>R. T. Senger and K. K. Bajaj, *Phys. Rev. B* **68**, 205314 (2003).